

Experimental observations and theoretical interpretation of anti-ballooning high-frequency Alfvénic activity in Wendelstein 7-AS

S. Zegenhagen¹, Yu.V. Yakovenko², Ya.I. Kolesnichenko², A. Werner¹, J. Geiger¹,
A. Weller¹, O.P. Fesenyuk²

¹ *Max-Planck-Institut für Plasmaphysik, D-17489 Greifswald, Germany*

² *Institute for Nuclear Research, 03680 Kyiv, Ukraine*

Introduction. Theoretical predictions [1–3] and experimental observations [4–6] show that the lack of toroidal symmetry in stellarators can result in the appearance of new types of Alfvén eigenmodes in the high-frequency part of the spectrum, namely, the helicity-induced and mirror-induced Alfvén eigenmodes (HAE and MAE). It was found recently [7] that such eigenmodes can be trapped in certain “waveguides” due to interference of several Fourier harmonics of the configuration. In this work, experimental observations of high-frequency Alfvénic activity in shot # 54937 of the stellarator Wendelstein 7-AS (W7-AS) are reported and compared with theoretical predictions.

High-frequency activity in W7-AS shot # 54937. At the final stage of shot # 54937, coherent high-frequency activity was observed. The frequency spectrum of the activity consisted of several lines in the range of 200–450 kHz (see Fig. 1), which well exceeded the frequencies of toroidicity- and ellipticity-induced Alfvén eigenmodes, TAEs and EAEs (less than 100 kHz in the plasma core). Each line seems to be produced by a separate instability since the amplitudes of the lines evolved independently. The identification of the instabilities as Alfvén eigenmodes is supported by the fact that their frequencies slowly increased with a decrease of the plasma density. The instabilities were detected by Mirnov coils, which included two poloidal arrays

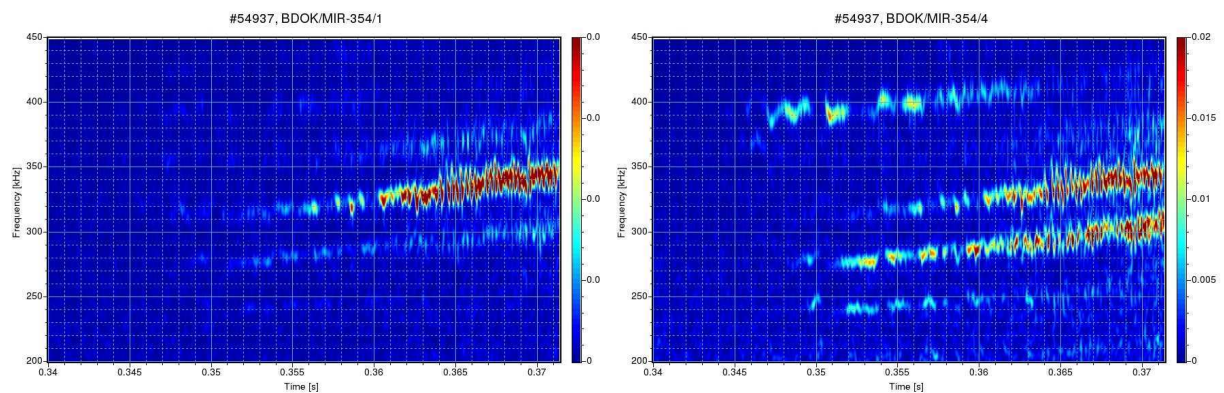


Figure 1: Frequency spectrum of Mirnov signals in W7-AS shot # 54937 vs time. Left panel, coil 1; right panel, coil 4.

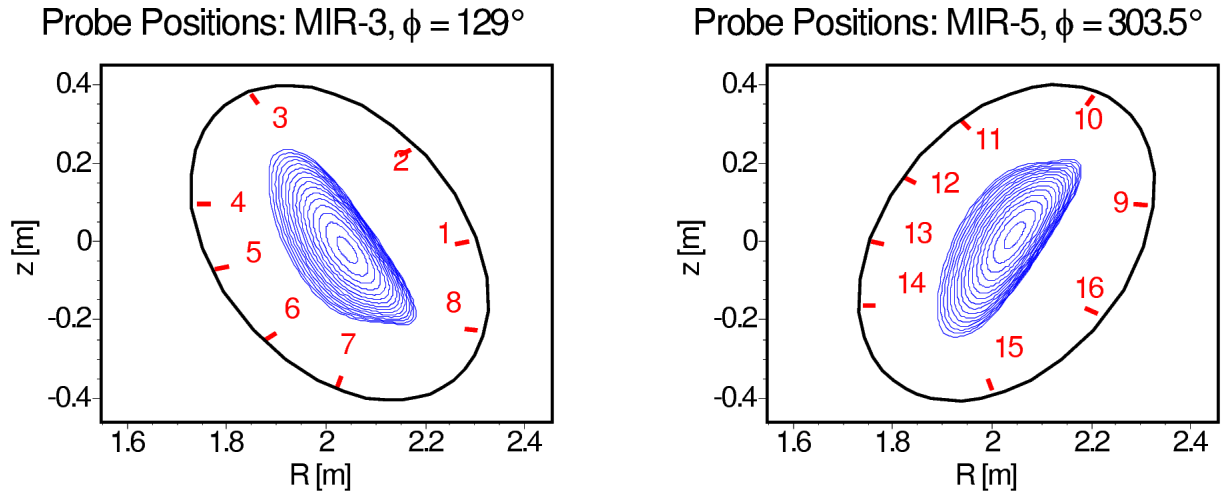


Figure 2: Locations of Mirnov coils.

located at the toroidal angles of $\phi = 129^\circ$ and $\phi = 303.5^\circ$ (see Fig. 2).

Comparison of the frequency spectra of the activity at different Mirnov coils reveals that the spectral lines exhibit different dependence on the poloidal angle, θ . Figure 1 shows the spectra of the signals on the coils 1 and 4 located on outer and inner circumferences of the torus, respectively. The comparison of the two spectra shows that most spectral lines (the lines with the frequencies about 250, 290 and 410 kHz at $t = 0.36$ s) are much stronger at the coil 4. The 320-kHz line has approximately equal amplitudes at both coils. In general, the dependence of the signal amplitude on θ was rather complicated, which may be partly explained by geometrical effects (including the variation of the distance between the plasma and the coils). Comparing the amplitudes of all spectral lines with that of the 320-kHz line confirms the pattern observed on the coils 1 and 4: Most spectral lines exhibit anti-ballooning behaviour in the sense that the signals almost vanish at the outer circumference.

Theoretical analysis. The Alfvén continuum (AC) code COBRA [2] was used to calculate the AC for $t = 0.36$ s. The results are shown in Fig. 3, where the gaps in the continuum are labelled by the corresponding coupling numbers (μ, ν) [the gap with the coupling numbers (μ, ν) results from coupling of wave harmonics with the poloidal and toroidal wave numbers (m, n) and $(m + \mu, n + \nu N)$, where N is the number of the field periods of the device]. The frequency range of interest corresponds to helicity-induced ($\mu \neq 0, \nu \neq 0$) and mirror-induced ($\mu = 0, \nu = 1$) gaps. The widest of them are the gaps $(2, 1)$ and $(3, 1)$ (the latter is not shown in Fig. 3), which result from the helical elongation and triangularity of the flux surfaces, respectively.

Let us consider the structure of Alfvén eigenmodes in this part of the spectrum. Applying the ballooning formalism described in [8] to the Alfvén wave equation [2], we obtain the following

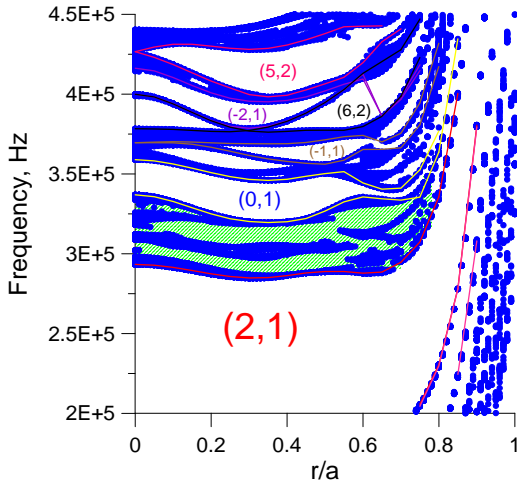


Figure 3: The Alfvén continuum in W7-AS shot # 54937. Blue dots, the continuum; the gaps are labelled with the corresponding numbers (μ, ν) . The region where the calculations are not reliable is hatched with green.

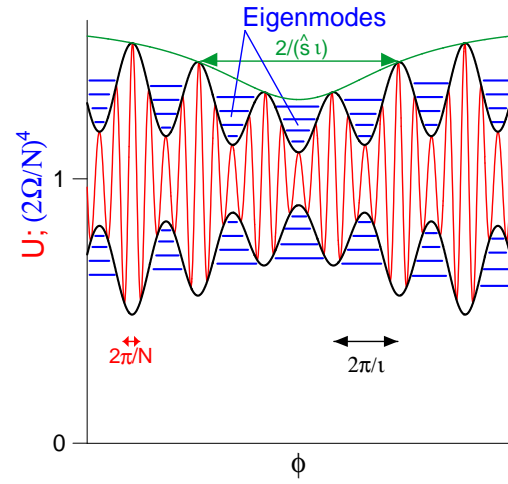


Figure 4: Sketch of the potential U in equation (3) and its bounded states. Thin red curve, U ; bold black curves, the envelopes of U ; blue lines, the frequencies and the localizations of eigenmodes.

equation, which determines the scalar potential of the electromagnetic field of the eigenmode (Φ) along a field line:

$$\frac{d}{d\phi} \left(D \frac{d\Phi}{d\phi} \right) + \Omega^2 \frac{D}{h_B^4} \Phi = 0, \quad (1)$$

where

$$D = h_g^{\theta\theta} + 2(\phi - \phi_k) \hat{s} t h_g^{\psi\theta} + (\phi - \phi_k)^2 \hat{s}^2 t^2 h_g^{\psi\psi}, \quad (2)$$

$\Omega = \omega R_0 / \langle v_A \rangle$, $\langle \dots \rangle$ denotes flux surface averaging, $h_B = B / \langle B \rangle$, $h_g^{\psi\psi} = g^{\psi\psi} / \langle g^{\psi\psi} \rangle$, $h_g^{\theta\theta} = g_{\perp}^{\theta\theta} / \langle g_{\perp}^{\theta\theta} \rangle$ and $h_g^{\psi\theta} = g^{\psi\theta} / (\langle g^{\psi\psi} \rangle \langle g_{\perp}^{\theta\theta} \rangle)^{1/2}$ are normalized metric tensor components, $g_{\perp}^{\theta\theta} = g^{\theta\theta} - (b^{\theta})^2$; g^{ij} with $i, j = \psi, \theta, \phi$ are the components of the contravariant metric tensor; b^{θ} denotes the corresponding contravariant component of $\mathbf{b} \equiv \mathbf{B} / B$, \mathbf{B} is the magnetic field, prime means differentiation in ψ , ϕ_k is a standard parameter of the ballooning formalism, which characterizes the transversal wave number.

We consider the frequency range of two adjacent helicity-induced gaps with the numbers $(\mu, 1)$ and $(\mu + 1, 1)$ and assume for simplicity that each of the dimensionless coefficients $h_g^{\psi\psi}$, $h_g^{\theta\theta}$, $h_g^{\psi\theta}$, and h_B includes only the corresponding two harmonics proportional to $\exp(i\mu\theta - iN\phi)$ and $\exp[i(\mu + 1)\theta - iN\phi]$. The substitution $\Phi = D^{-1/2} \hat{\Phi}$ transforms equation (1) into a Schrödinger-type equation:

$$\frac{d^2 \hat{\Phi}}{d\phi^2} + \Omega^2 U(\phi) \hat{\Phi} = 0, \quad (3)$$

with the potential U schematically shown in figure 4 for the case of $N \gg l$. The potential pos-

sesses three characteristic scales in ϕ . The smallest one, $\Delta\phi \sim 2\pi/N$, is approximately the period of each harmonic. The second one, $\Delta\phi \sim 2\pi/\iota$, is the period of the beatings associated with the presence of two harmonics with close periods along the field lines. The third one, $\Delta\phi \sim 2/(\iota\hat{s})$, is the characteristic scale that usually appears in the ballooning theory. Averaging over the fast oscillations shows that the eigenmodes of equation (3) are localized in the “pockets” of the envelope, which are the places where the net amplitude of the two harmonics is minimum. For instance, the Helicity-induced Alfvén Eigenmodes (HAEs) produced by the Fourier harmonics with $(\mu, \nu) = (2, 1)$ and $(3, 1)$ are typically localized at the inner circumference of the torus, which is determined by the signs of the corresponding harmonics of the configuration (in general, other localizations are also possible, see [7]).

This result well agrees with the experimental fact that most high-frequency spectral bands are much better observed by the coils located at the inner circumference of the torus. The 320-kHz frequency band, which shows no signs of anti-ballooning localization, falls in the range of the strong interaction gaps with different values of ν [e.g., the $(1, 1)$ - and $(7, 0)$ -gaps, which lie near 320 kHz]. This means that the waveguides of this eigenmode could have a more complicated shape, which would explain the absence of poloidal trapping. However, one cannot rule out another explanation of the absence of poloidal trapping because we do not allow for the plasma rotation, which could be fast in this shot due to non-balanced NBI heating and might shift the frequencies of the modes.

Conclusions. The strong poloidal inhomogeneity of the high-frequency Alfvénic activity in shot # 54927 of W7-AS can be explained by the poloidal trapping of Alfvén waves due to interference of elongation and triangularity of the flux surfaces. Further development of theory is required to find the radial localization of the modes and their Fourier spectrum.

References

- [1] N. Nakajima, C.Z. Cheng and M. Okamoto, Phys. Fluids B **4**, 1115 (1992)
- [2] Ya.I. Kolesnichenko et al., Rep. IPP III/261 (2000); Phys. Plasmas **8**, 491 (2001)
- [3] C. Nührenberg, ISSP-19 “Piero Caldirola”, Theory of Fusion Plasmas (2000), p. 313
- [4] S. Yamamoto et al., 29th EPS Conf. on Plasma Phys. and Control. Fusion, Montreux, 2002, Europhys. Conf. Abstr. **26B** (2002), Rep. P1.079
- [5] V.V. Lutsenko et al., Fusion Energy 2002, 19th Conf. Proc., Lyon (IAEA, 2003) Rep. TH/P3-15
- [6] A. Weller et al., Plasma Phys. Control. Fusion **45**, A285 (2003)
- [7] Yu.V. Yakovenko et al., Proc. 13th Int. Congr. on Plasma Phys., Kiev, 2006, Report B022p
- [8] R.L. Dewar and A.H. Glasser, Phys. Fluids **26**, 3038 (1983)